

**Analysis of the Swimming-to-Crawling Transition of *Caenorhabditis elegans* in
Viscous Fluids**

by

RISA KAWAI

Submitted to the Department of Physics in partial fulfillment of the Requirements for the
Degree of

BACHELOR OF SCIENCE

at the

MASSACHUSETTS INSTITUTE OF TECHNOLOGY

June 2008

© 2008 RISA KAWAI

All Rights Reserved

The author hereby grants to MIT permission to reproduce and to distribute publicly paper and
electronic copies of this thesis document in whole or in part.

Signature of Author _____

MIT Department of Physics

May 9, 2008

Certified by _____

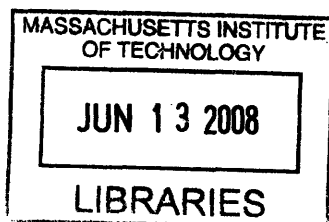
Professor Sebastian Seung

Thesis Supervisor, MIT Department of Physics

Accepted by _____

Professor David E. Pritchard

Senior Thesis Coordinator, MIT Department of Physics



ARCHIVES

Analysis of the Swimming-to-Crawling Transition of *Caenorhabditis elegans* in
Viscous Fluids

by

Risa Kawai

Submitted to the Department of Physics on May 9, 2008,
in partial fulfillment of the requirements for the Degree
of Bachelor of Science in Physics

Abstract

The locomotory behavior of the nematode *Caenorhabditis elegans* is often characterized by two distinct gaits – swimming when in fluids and crawling when on surfaces. Swimming is characterized by about a twice greater wavelength and about four time greater frequency of undulatory waves, compared with the crawling gait. These mechanisms which generate these gaits are not well-understood but have been suggested to be controlled by two separate neural circuits of central pattern generators. Here we studied the locomotion of young adult *C. elegans* in viscous fluids ranging from 0.001-1000 Pa s to determine whether there is a sharp or continuous transition between swimming and crawling. We characterized the locomotion by two parameters: the wavelength and the frequency of the undulating gaits. Our results for both parameters show a smooth transition, which suggests that there is only one neural circuit controlling forward locomotion which is modulated by the mechanical loading of the environment.

Thesis Supervisor: Professor Sebastian Seung

Title: Thesis Supervisor, MIT Department of Physics

Thesis Supervisor: Professor Aravinthan Samuel

Title: Thesis Supervisor, Harvard Department of Physics

Acknowledgments

I would like to express my gratitude to everyone who helped me with this thesis project and since this senior thesis marks the end of my undergraduate career, I would also like to take this opportunity to express my gratefulness to those who have supported and guided me throughout my time at MIT.

First and foremost, I am indebted to Professor Sebastian Seung for being my thesis advisor and my UROP supervisor for the past 3 years. He has always been willing to answer my questions despite his busy schedule. I also thank him for introducing me to biophysics and neuroscience, the fields that I have decided to pursue for graduate school. Finally, I thank him for giving me the opportunity to participate as a lab member.

I would also like to thank Professor Aravinthan Samuel for letting me conduct research in his lab. He is always encouraging and has given me this amazing chance to learn more about biophysics.

Dr. Christopher Fang-Yen mentored me throughout my senior thesis and taught me everything from picking worms to building video setups. Without him, this project would not be where it is now and am grateful for helping me for this semester.

The past two years of UROP projects is attributed to Neville Sanjana, for giving me so much guidance. He let me take over his rig and practically his office, where I learned the most essential tools for being a scientist. Neville has taught me more than any class than I could ever take. Not only did he help me with science, but he took the time to help me with graduate school applications and decisions.

Nothing in Seung Lab would be possible without Amy Dunn. She is the most prompt and organized person I have ever met and am truly thankful for all of the work she does behind the scenes.

Thanks to Jeannine Foley and John Choi for making the best neuron cultures. The successes of experiments are ascribed to them.

Many thanks to Dr. Sen Song for spending a whole summer with me and being patient as we sought the elusive LTP.

The graduate students and post-docs in Seung Lab were very supportive during my frantic search of graduate school. Thanks to Viren Jain, Srinu Turaga, Dr. Uri Rokni, and Jen Wang for giving me advice and for getting me in touch with people across the nation for grad school.

And finally, thanks to Dr. Artem Starovoytov for taking me under his wing during my freshmen year. He taught me what a neuron is and how to patch clamp. He is the reason why I am where I am today.

Table of Contents

| | |
|--|----|
| Chapter 1 Introduction | 7 |
| 1.1 Central Pattern Generators | 7 |
| 1.2 <i>Caenorhabditis elegans</i> | 8 |
| Chapter 2 Materials and Methods | 11 |
| 2.1 Strains and Staging | 11 |
| 2.2 Hypromellose..... | 12 |
| 2.3 Rheology | 13 |
| 2.4 Video analysis | 18 |
| Chapter 3 Results | 20 |
| Chapter 4 Discussion | 22 |
| Chapter 5 Appendix | 23 |
| 5.1 Dextran solution | 23 |
| 5.2 Mutants | 24 |
| Chapter 6 Bibliography | 26 |

Chapter 1

Introduction

1.1 Central Pattern Generators

Many animals travel by means of undulating propulsion. For example, lampreys swim through water, and snakes crawl or glide on land. For many of these animals, the oscillatory motion is controlled by neural networks known as central pattern generators (CPGs). CPGs are circuits that endogenously produce rhythmic outputs. CPGs are not limited to locomotion and are proposed to control a wide variety of rhythmic behaviors including chewing, swallowing, and breathing [1] [2]. The classic example is the stomatogastric ganglion of spiny lobsters. The gastric mill motor system drives three internal teeth to rhythmically move for food mastication [3]. The CPG circuit is shown in Figure 1-1A. The stomatogastric ganglion is one of the simplest CPGs, and the neurons and the types of synapses within the circuit have been determined. The extracellular recordings of motor nerves of an isolated stomatogastric nervous system show the rhythmic bursting output, even without sensory input (See Figure 1-1B). Although much progress has been made in this system, the circuit dynamics and neuromodulation are still not yet fully understood.

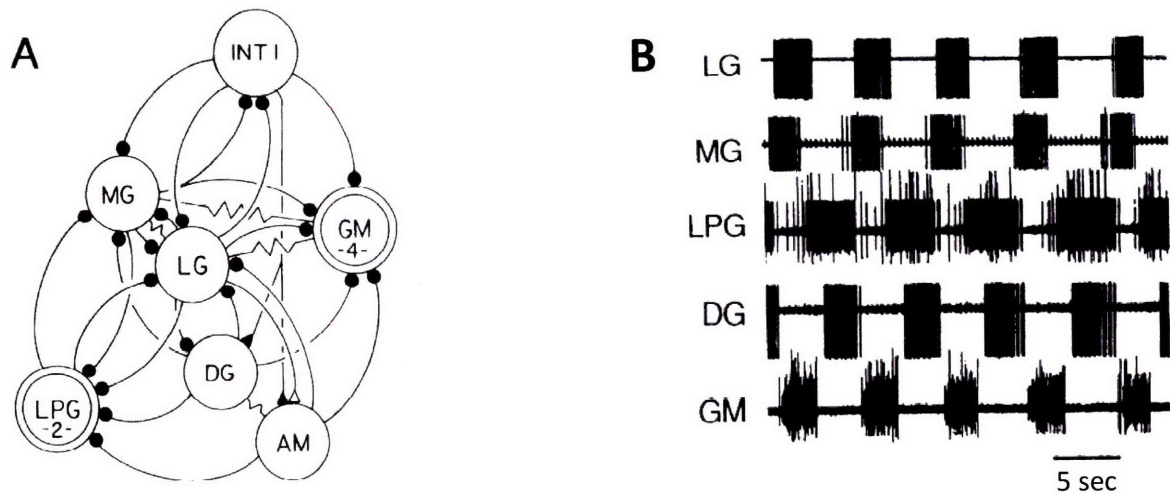


Figure 1-1 From [3] (A) Network connectivity of the stomatogastric ganglion. (B) Extracellular recordings of motor nerves. LG = lateral gastric motor neuron; MG = medial gastric motor neuron; LPG = lateral posterior gastric motor neurons; DG = dorsal gastric motor neurons; GM = gastric mill motor neurons; AM = anterior median motor neuron; INT = interneuron; Synapses: filled circles, chemical inhibitory; filled triangles, chemical excitatory; open triangles, functional excitation; resistor symbol, electronic coupling

An animal with identified locomotory CPGs is the leech. Leeches can travel through fluids by swimming and on land by crawling. Their central nervous system (CNS) has been studied, and two CPGs have been discovered, one for swimming and one for crawling [4] [5]. Besides having rhythmic output, CPGs are unique because they can produce an output even without any sensory input [1]. For instance, in the leech, an isolated nerve cord electrically initiated can produce a crawling motor pattern without sensory input [4]. Sensory input can however help modulate the rhythmic behaviors for environmental perturbations, such as adjusting body curvature to go around a reed in a pond in the leech.

While many CPGs have been proposed, besides the leech, there are very few unambiguous experiments that have identified true CPGs. We still do not have much understanding of the circuitry of CPGs, how sensory feedback contributes to CPGs, or how CPGs generate behavior [6].

1.2 *Caenorhabditis elegans*

The nematode *Caenorhabditis elegans* serves as a model for studying locomotory behavior. Studying *C. elegans* has several advantages. First, *C. elegans* is anatomically one of the simplest multicellular organisms. The nervous system of *C. elegans* contains exactly 302 neurons, for which the full connectivity wiring diagram has been determined [7] [8], and 959 somatic cells, for which the full cell lineage has been determined [7] [9]. The second advantage is that there are numerous genetic techniques available for *C. elegans*. The genome has been completely sequenced, allowing for specific knockouts, mutagenesis and genetic manipulations. Lastly, *C. elegans* has stereotyped locomotory gaits. In fluids, the worms “swim”, as shown in Figure 1-2.

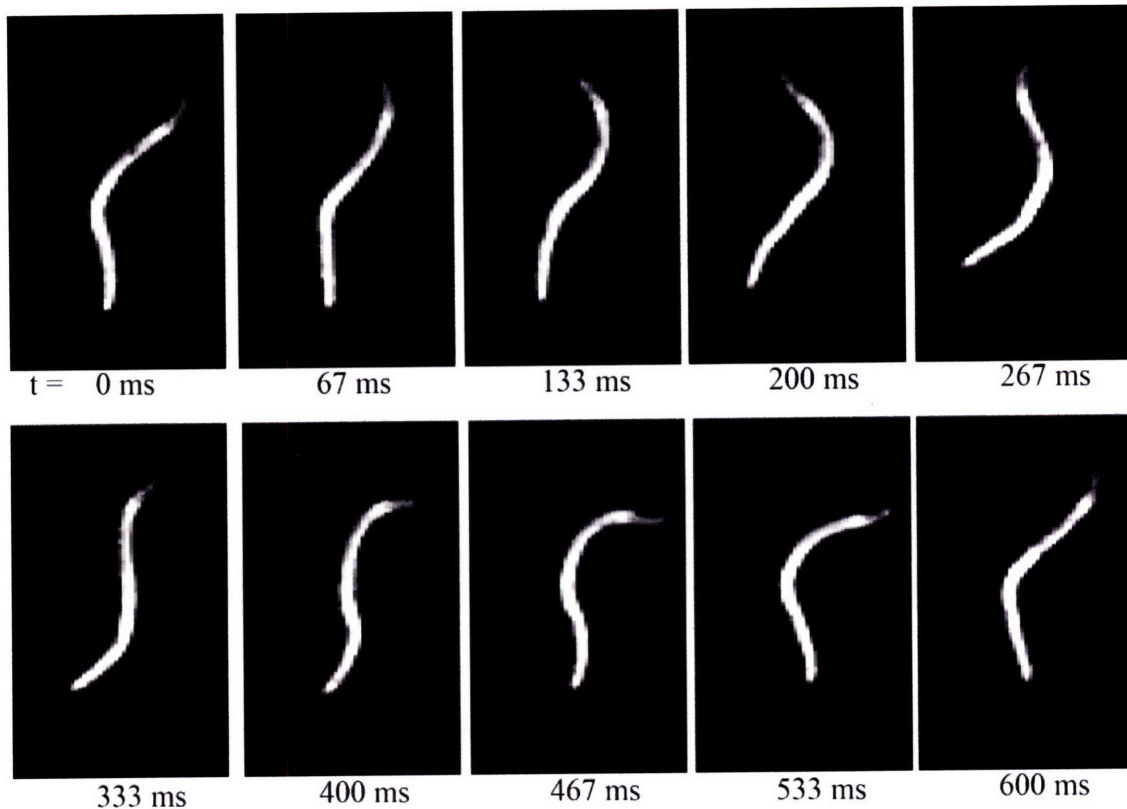
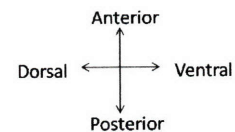


Figure 1-2 *C. elegans* swimming in Nematode Growth Medium (NGM)



On agar surfaces or in viscous fluids, the worms “crawl” as shown in Figure 1-3. In swimming and crawling, the worm moves forward by propagating a wave along the anterior-posterior¹ axis in the dorsal-ventral plane. The waveform and frequency of the undulations, however, are different from each other. Swimming *C. elegans* have frequencies in the range of 1.5 to 2 Hz and have normalized wavelengths (wavelength/body length) in the range of 1 to 1.5. Crawling *C. elegans* have frequencies in the range of 0.2 to 0.4 Hz and have normalized wavelength in the range of 0.4 to 0.7. The two forms of locomotion seem to be distinct. No CPG for locomotion has been identified in *C. elegans*, but it has been suggested on the basis of genetic evidence that the two forms of locomotion, swimming and crawling, are controlled by different CPGs.

¹ Anterior refers to the head end, posterior refers to the tail end, dorsal is the back, ventral is the belly

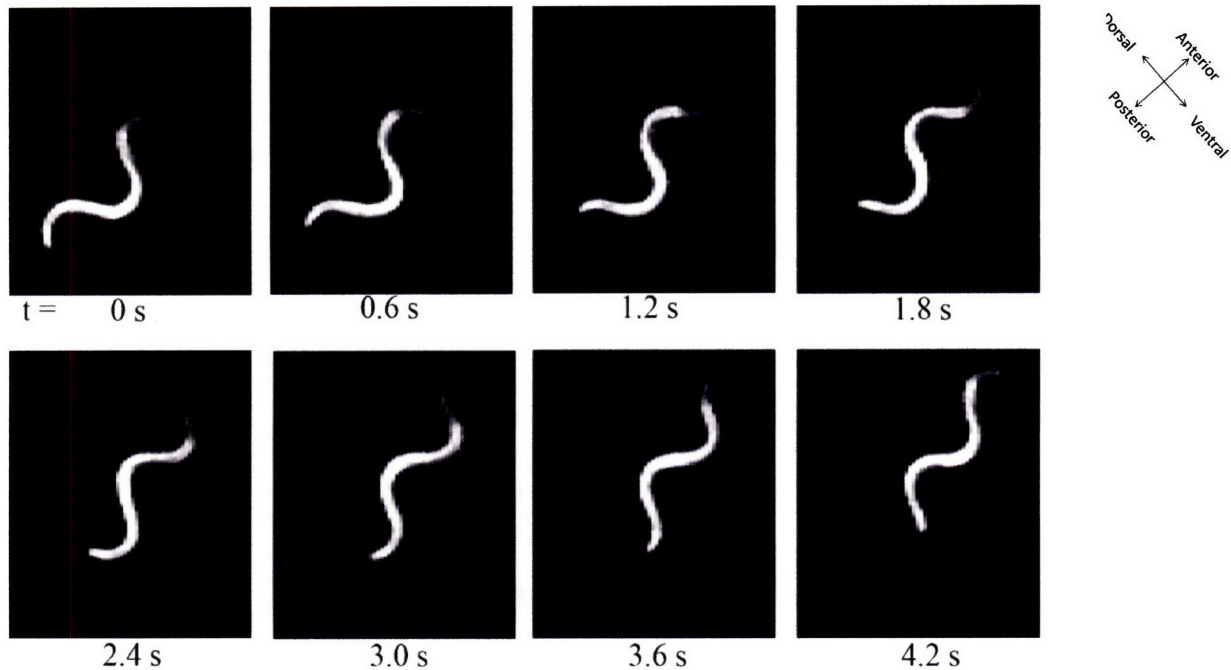
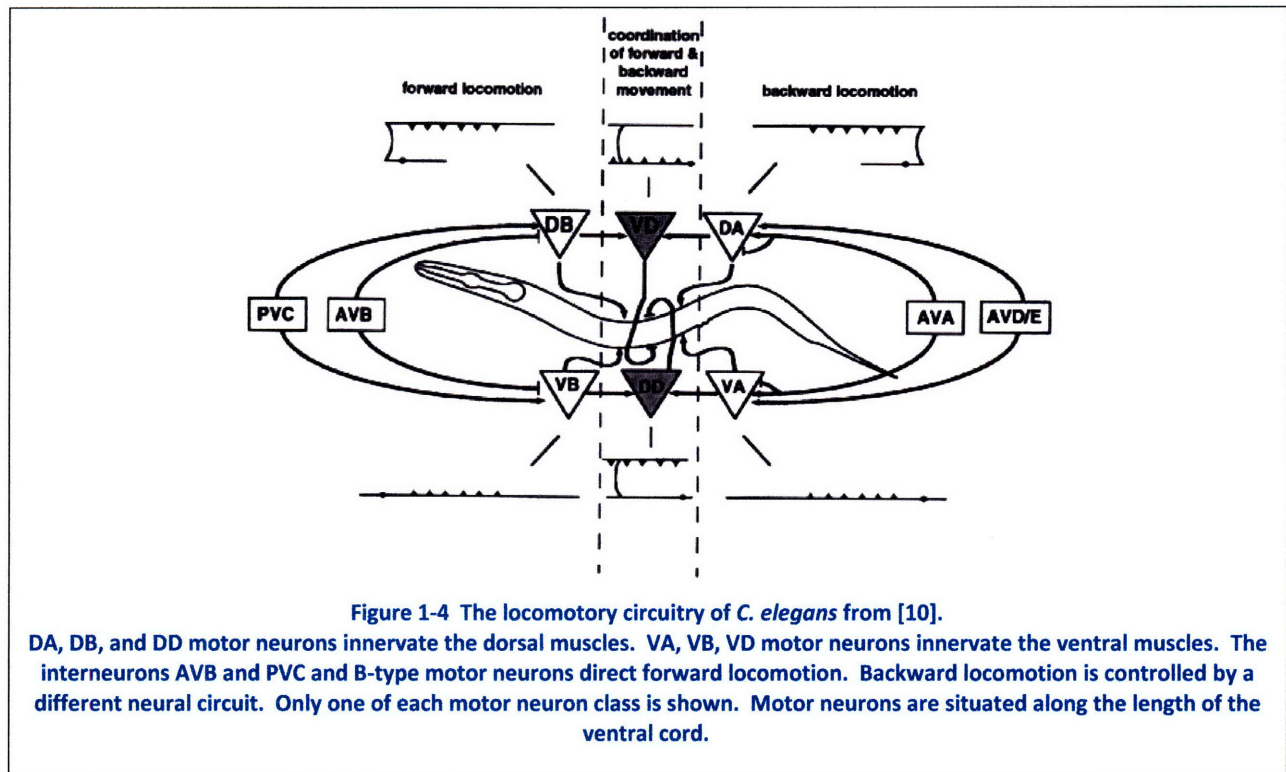


Figure 1-3 *C. elegans* crawling in a viscous fluid (3.6% hypromellose in NGM)

Not all rhythmic locomotory behavior is controlled by CPGs. Oscillatory patterns can also be generated by sensory input, and it is not implausible that *C. elegans* do not have any CPGs for forward locomotion. Stretch receptors and other mechanosensory neurons have been shown to play a significant role in forward locomotion and it has not yet been established whether these neurons act as modulators in CPGs or are the driving inputs in a pattern-generating neural circuit (See Chapter 4).

C. elegans move via two dorsal rows and two ventral rows of body wall muscles. Distinct classes of motor neurons control the dorsal and ventral body muscles. The DA, DB, DD motor neurons innervate the dorsal muscles, and the VA, VB, and DD neurons innervate the ventral muscles, as shown in Figure 1-4. The dorsal and ventral body muscles contract out of phase to produce the sinusoidal pattern of movement. Little is known how the rhythmic pattern is initiated. In other known CPGs, individual cells that have intrinsic oscillating output begin the oscillations. No such neurons have been found in *C. elegans* so far. Little is also known about how the wave propagates along the body. Adjacent muscle cells or adjacent motor neurons coupled by electrical gap junctions could promote wave propagation. An

alternative possibility is that the motor neurons act as stretch receptors such that the body muscle contractions themselves regulate motor neuron activities [10].



To experimentally test whether there are two distinct neural circuits, we studied the locomotory gaits of *C. elegans* in fluids with viscosity ranging from 0.001 Pa s to 1000 Pa s. If there are two circuits, we would expect that at low viscosities, the worms should swim. At some critical viscosity, a sharp transition to crawling should occur, and at all higher viscosities, the worms should crawl. Here we analyzed the worms' movements to characterize the effects of mechanical load on locomotion.

Chapter 2 Materials and Methods

2.1 Strains and Staging

Caenorhabditis elegans wild-type Bristol N2 were maintained at 20°C using standard methods [11]. Selected worms were young adult hermaphrodites. Staging was done in either one of two ways. The first way was by selecting the larval stage L4 (identified by the crescent-shaped immature vulval

structure) the night before experiments were conducted. The second way was bleaching the worms 3 days before the day that experiments were conducted. In the bleaching process, only the eggs survive, insuring that all of the worms are the same age differing at most by several hours. The life cycle of *C. elegans* is shown in Figure 2-1. The number of worms from the same generation used in experiments was at most 3 worms.

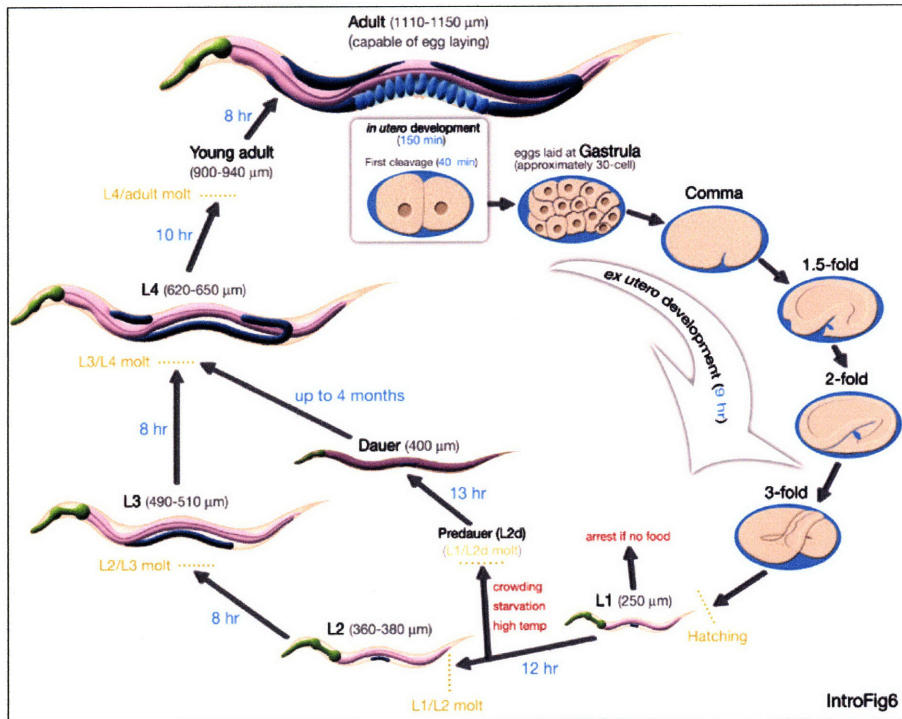


Figure 2-1 The life cycle of *C. elegans* at 22°C [7]. Staging was done by either picking L4s the night before or bleaching adult worms with eggs ~3 days before experiments. (Note: The life cycle depends on temperature. Our worms were kept at 20°C and therefore develops more slowly than shown above.)

2.2 Hypromellose

Stock solutions of viscous fluids were prepared by adding hypromellose (Benecel® by Hercules-Aqualon [12]) to Nematode Growth Medium (NGM) [13]. Hypromellose (short for hydroxypropyl methylcellulose, also known as HPMC) is a viscoelastic polymer, used in pharmaceutical and commercial products. We used a rheometer to determine the viscoelasticity of each of our solutions.

2.3 Rheology

Rheology is the study of deformation and flow of materials under external forces, and a rheometer measures the response of a fluid due to applied forces, such as shear strain and shear stress [14]. When a force F is applied to a fluid of thickness H , the shear stress τ is defined as

$$\text{Shear Stress} = \tau = \frac{F}{A}, \quad (1)$$

where A is the tangential area, and the shear strain γ is defined as

$$\text{Shear Strain} = \gamma = \frac{D}{H}, \quad (2)$$

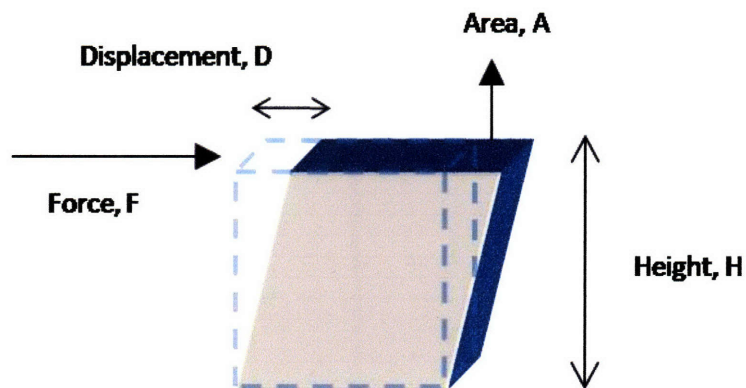


Figure 2-2 Shear Stress and Strain

where D is the displaced distance (See Figure 2-2). The rate of shear deformation is called the shear rate. Viscous fluids are resistant to being deformed by shear stress. Elastic materials deform under shear stress and return to its original shape when stress is removed. Viscoelastic fluids are materials that exhibit some of both of these properties.

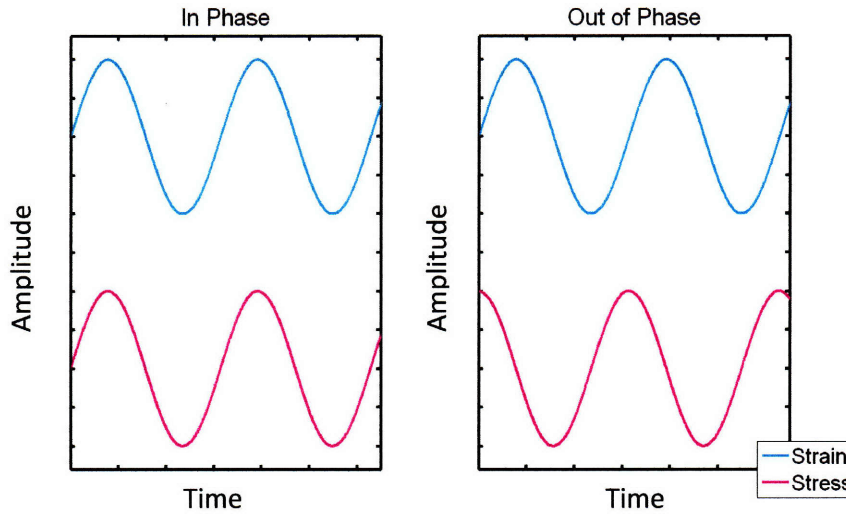


Figure 2-3 Left: Perfectly elastic -- strain and stress are in phase Right: Viscoelastic -- strain and stress are out of phase

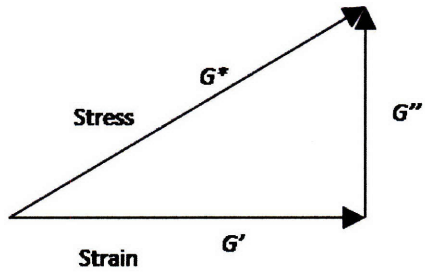


Figure 2-4 Complex Rigidity Modulus: Viscoelastic fluids under sinusoidal time-varying stress can be represented by strain and stress components

When a fluid undergoes sinusoidal time-varying stress, the shear strain also responds sinusoidally, but not necessarily in phase (See Figure 2-3). Purely elastic materials are exactly in phase and purely viscous materials are out of phase by 90°. Viscoelastic fluids have a phase difference in between 0° and 90°. By convention, strain and stress are

separated into two components, as in Figure 2-4:

$$G'(\omega) = \frac{\text{component of stress in phase with strain}}{\text{strain}} = \text{Storage or Elastic Modulus}, \quad (3)$$

$$G''(\omega) = \frac{\text{component of stress in } 90^\circ \text{ out of phase with strain}}{\text{strain}} = \text{Loss or Viscous Modulus}, \quad (4)$$

where ω is the sinusoidal frequency. Together they define the complex rigidity modulus:

$$G^*(\omega) = G'(\omega) + iG''(\omega) \quad (5)$$

Complex (dynamic) viscosity is defined as

$$\eta^*(\omega) = \frac{G'(\omega)}{i\omega} = \eta' - i\eta'', \quad (6)$$

where η' represents viscosity and η'' represents elasticity [15] [16] [17].

We used a cone and plate rheometer (AR_G2, TA Instruments, New Castle, DE) to measure the viscosity and elasticity of our hypromellose solutions. Cone and plate rheometers have an advantage over other rheometers, such as the rotational cylinder rheometer, since the shear rate $\dot{\gamma}$ is uniform over the sample if the cone is shallow (i.e. if the angle between the cone and the sample, α , is very small) (See Figure 2-5). This can be shown by the following. Linear velocity at radius r is ωr . The gap width at radius r is $r \tan \alpha$. The shear rate at radius r is thus

$$\dot{\gamma} = \frac{\omega r}{r \tan \alpha} = \frac{\omega}{\tan \alpha} \approx \frac{\omega}{\alpha} \quad (7)$$

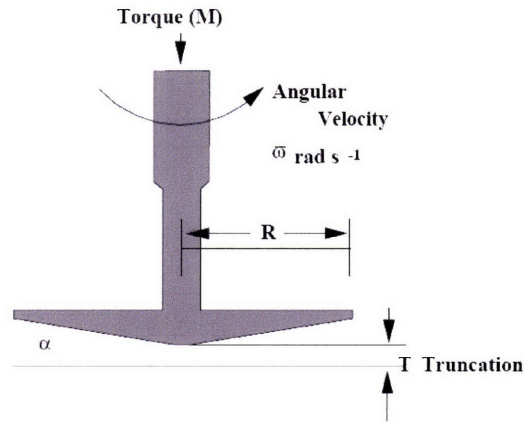


Figure 2-5 Cone and plate by TA Instruments [18]

Since the shear rate is constant over the sample, the apparatus can directly measure the viscosity and elasticity by oscillations.

The modulus and dynamic viscosity parameters are shown for our stock solutions as a function of frequency $f = \frac{\omega}{2\pi}$. The percentages correspond to the percentage by mass of hypromellose in the solution. We find that the solutions are highly non-Newtonian since there is an elastic component, and the viscoelasticity is not constant as a function of frequency. However, within the frequency regime of the swimming and crawling of the worms (0.1 Hz to 5 Hz), the viscosity and elasticity do not overlap from one concentration of hypromellose to another concentration of hypromellose. To test if the non-Newtonian properties affect the swimming and crawling behavior, we also tested the worms in stock solutions of dextran (Sigma, St. Louis, MO) in 10mM Hepes (Sigma) buffer (See Appendix). We chose to use the hypromellose solution over the dextran solution, however, due to the large osmotic changes for

high concentrations of dextran. High osmolality affects the health of the worms, and the worms shrink in volume [19] [20], which could affect the worms' locomotory properties.

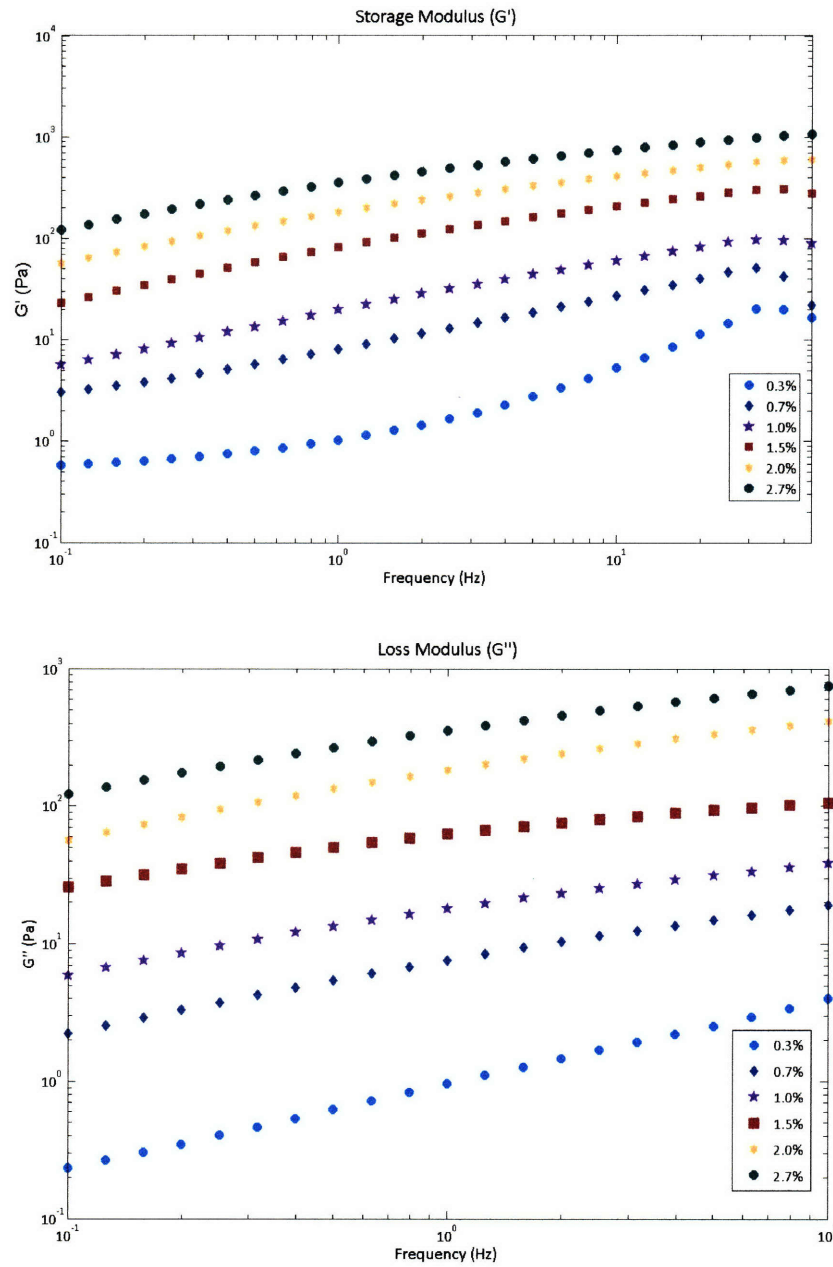


Figure 2-6 Top: The storage or elastic modulus, Bottom: The loss or viscous modulus
The undulations of C. elegans ranges from 0.1 Hz to 5 Hz.

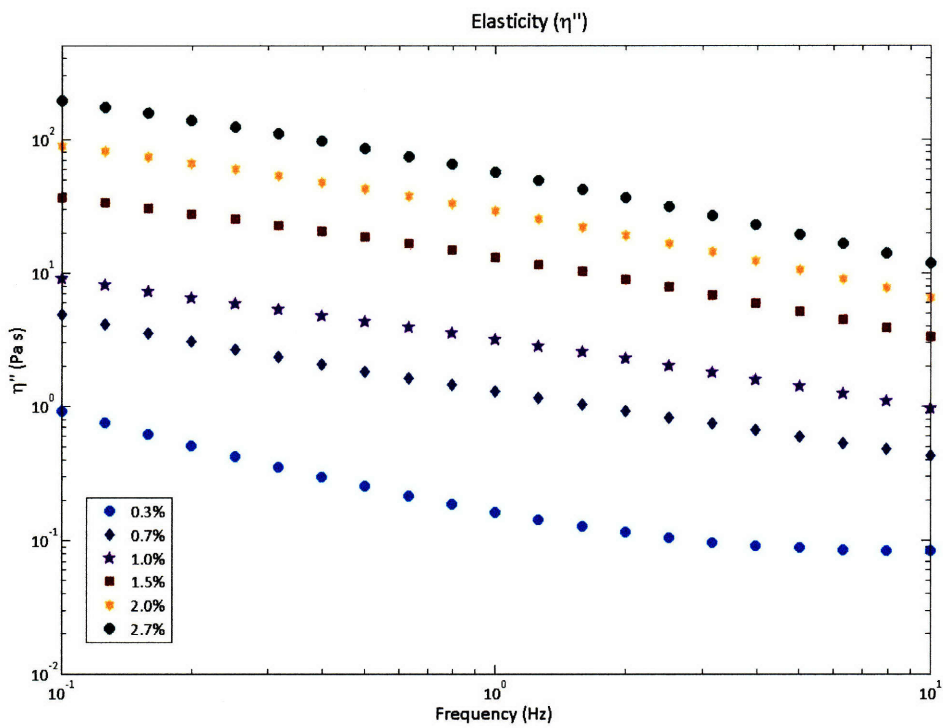
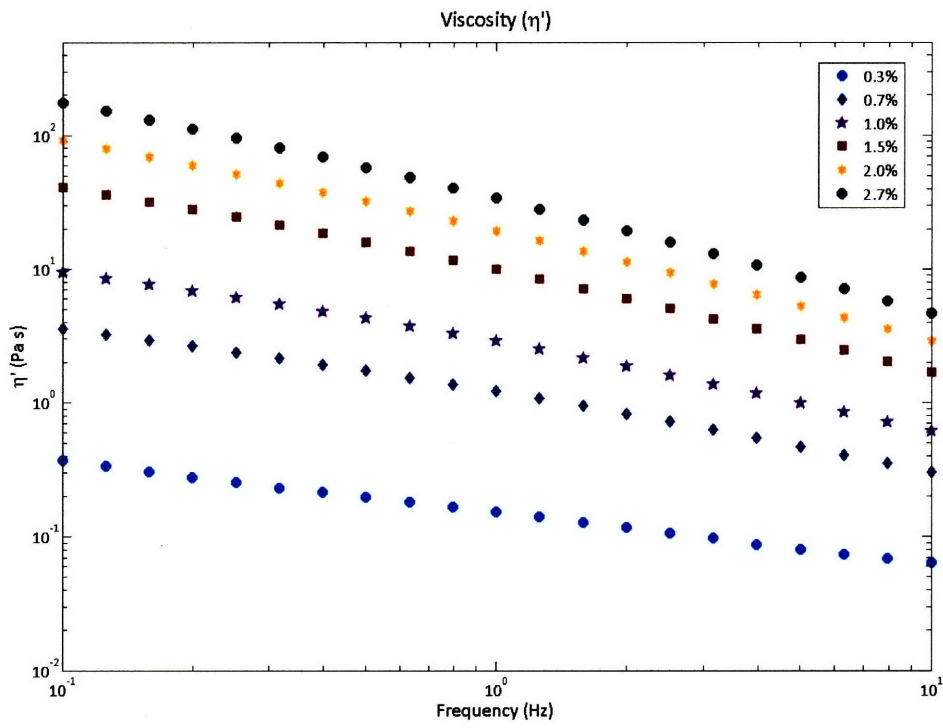
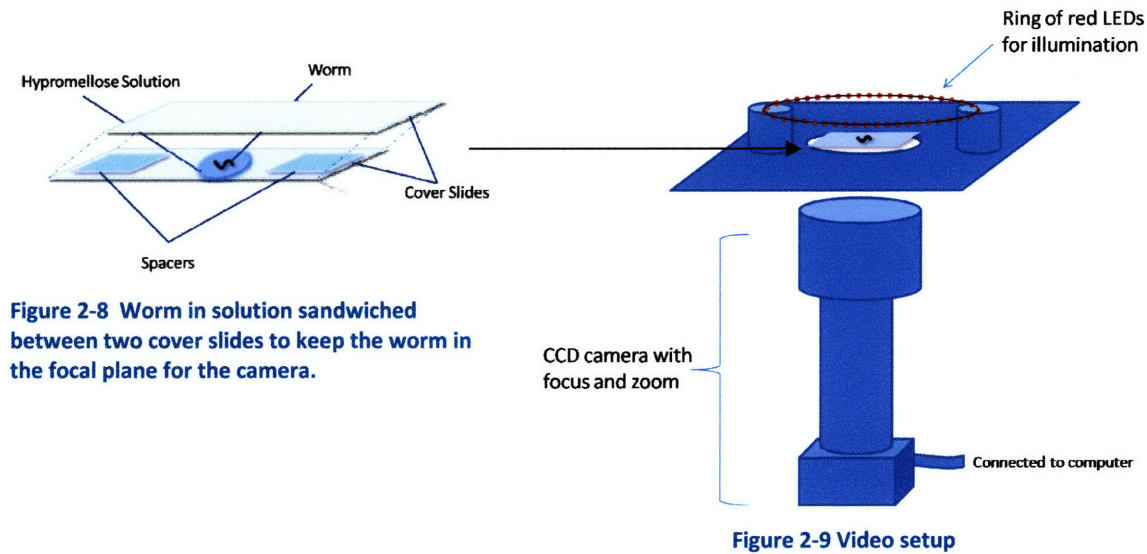


Figure 2-7 Top: Viscosity, Bottom: Elasticity

2.4 Video analysis

Worms were prepared for imaging by being rinsed in NGM buffer and placed into the hypromellose solution sandwiched between two cover slides. The cover slides prevent the worm from traveling in 3d motions and keep the worm in the focal plane for acquiring images with the camera. The worm was obliquely illuminated to produce a sharp contrast image of the worm's body against a dark background. A CCD camera was used to acquire images at 30 Hz for low viscosities (0% - 1.0% hypromellose) and 10 Hz for higher viscosities (1.5% - 3.6% hypromellose). See Figure 2-8 and Figure 2-9.



The frames were analyzed with an algorithm from [21] and a Matlab script written by Dr. Christopher Fang-Yen. An edge-detection algorithm was used to identify the x-y coordinates for all points along the dorsal and ventral sides of the worm. The dorsal and ventral edges were least squares fit with a continuous Bezier spline (degree 5, 12 points, open uniform knot). The center of the worm was found by taking the bisection of the vector connecting the dorsal side to the near point on the ventral side. This centerline was fit to a Bezier spline and divided into $N = 100$ evenly spaced points from the nose to the tail of the worm to define the worm in coordinates $[x_i(t), y_i(t)]$, where $i = 1$ to N , for all frames.

The curvature at each point was calculated by using the centerline coordinates. Curvature is defined as

$$\kappa = \frac{d\varphi}{dl}, \quad (8)$$

where φ is the tangential angle and l is the arc length. The tangential angle in terms of our coordinates is given by

$$\varphi_i = \tan^{-1} \left(\frac{y_i - y_{i-1}}{x_i - x_{i-1}} \right). \quad (9)$$

To make calculations easier, we define a body coordinate l along the centerline with the head of the worm having the coordinate $l = 0$ and the tail having the coordinate $l = L$, as shown in Figure 2-10.

To determine the properties of the locomotory gait, we analyzed the curvature at each point along the body of the worm for each frame. As shown in Figure 2-11, we can determine the period (the time from one undulation to the next) and the wave speed (the rate of propagation of the curvature down the length of the body). By using the relation, wavelength = period x wave speed, we also determined the wavelength of the undulation. A minimum of 4 wave cycles per worm was used for calculations.

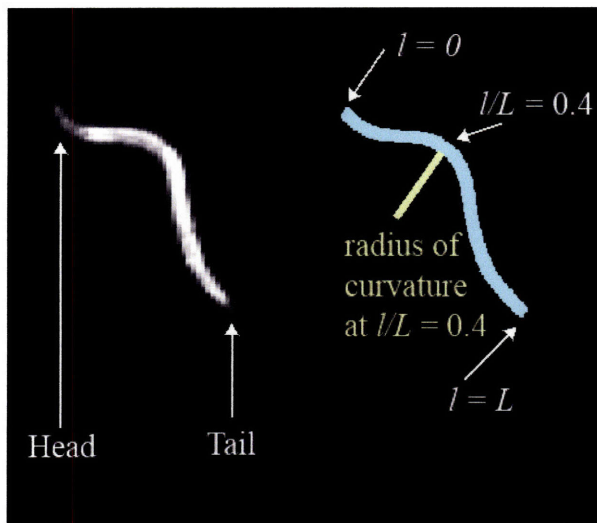


Figure 2-10 The worm was fit with a Bezier spline. The curvature was calculated at each point (total of 100 points). The body coordinate l is defined as 0 for the head and L for the tail. This worm is in 0.7% hypromellose solution.

Contour Plot of Spatiotemporal dynamics

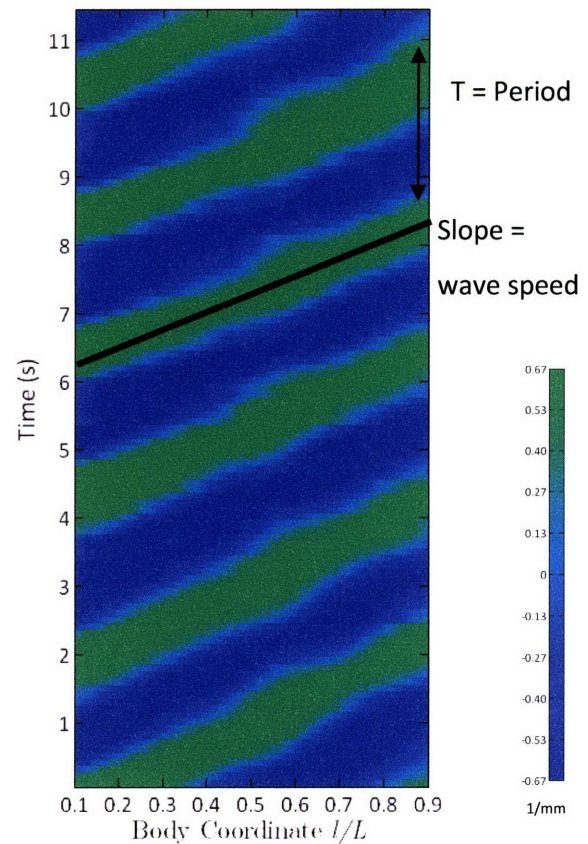


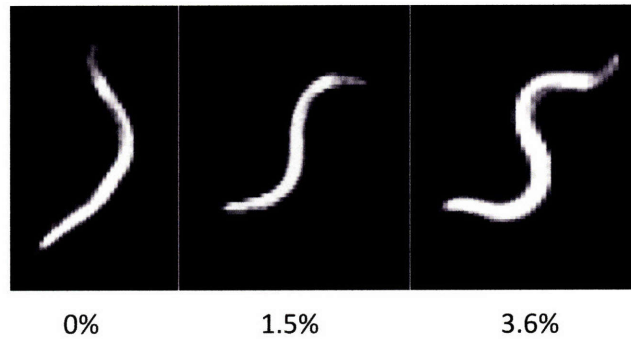
Figure 2-11 The contour plot represents the curvature along the body of the worm over time. Green indicates curvature in one direction (i.e. dorsal) and blue indicates curvature in the other direction (i.e. ventral). From the slope of each stripe, we can determine the wave speed of the locomotory undulation. From the distance between two consecutive same-colored streaks, we can determine the period or frequency of the undulation. Here we show the data from $l/L = 0.1$ to 0.9 to exclude the nose and tail, which are more flexible than the rest of the body. The calculations for this plot were for a worm in 1.5% hypromellose solution.

Chapter 3

Results

The results for the locomotory gait of wild type N2 *C. elegans* is shown in Figure 3-2. The two parameters we present are wavelength (λ) and frequency ($1/T$). The wavelength was normalized to the worm's total body length L . For both parameters, we observe a smooth decrease with increasing concentrations of hypromellose.

Figure 3-1 The worm's wavelength and frequency of undulations smoothly changes with viscosity.



As shown previously, solutions with higher concentrations of hypromellose are more viscous. Thus, wavelength and frequency decrease with higher mechanical load. Here we chose to plot the parameters against concentration rather than viscosity since our solutions are non-Newtonian fluids, meaning the viscosity dependent on several factors including the velocity of the worm. Although swimming and crawling are characterized to be two distinct locomotory behaviors, there does not appear to be a transition from the swimming gait to the crawling gait.

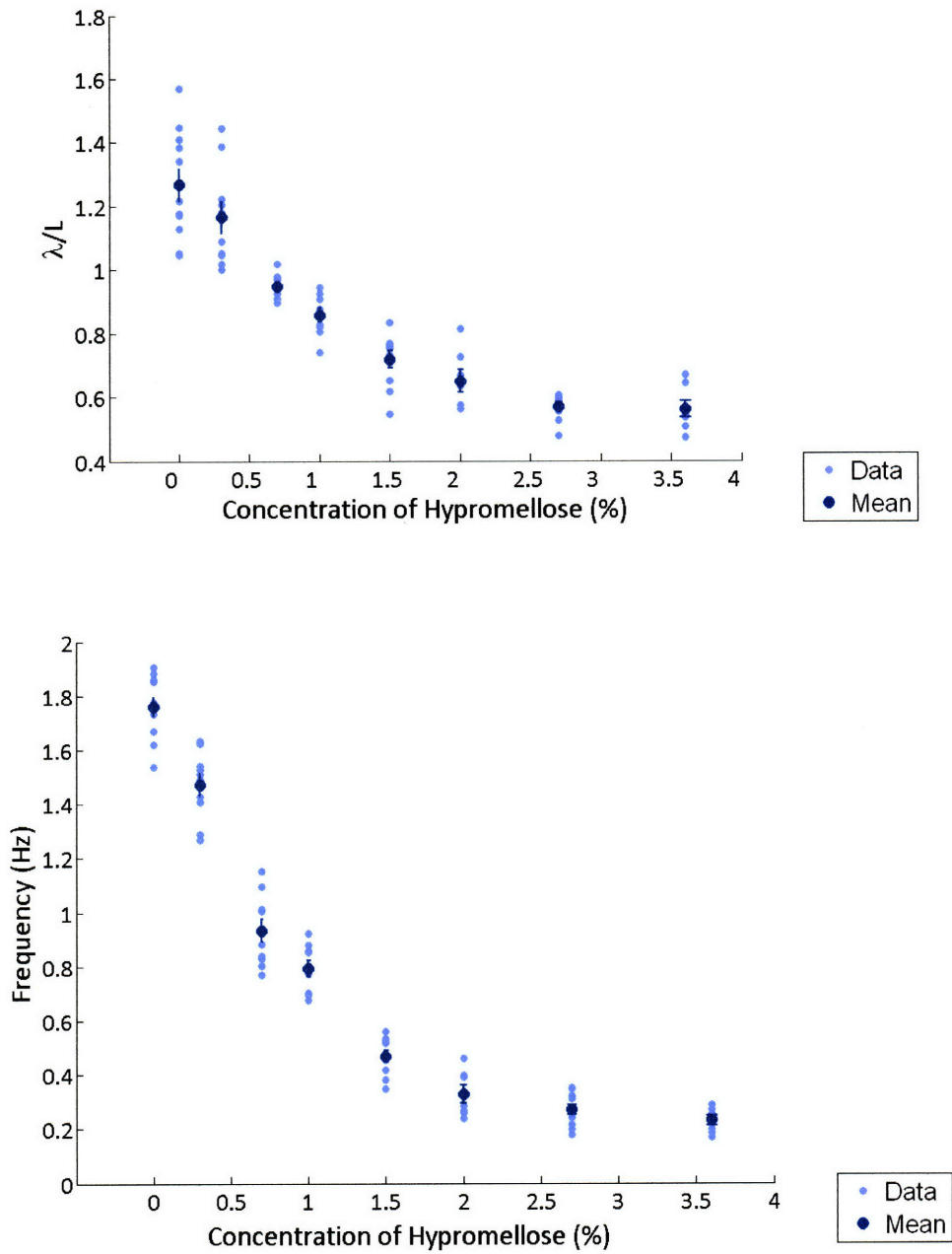


Figure 3-2 Top: Wavelength of the undulation vs. concentration of hypromellose solution. The wavelength is normalized by the length of the worm's body. Bottom: Frequency of the undulation vs concentration of hypromellose solution. The means (\pm s.e.m.) correspond to the data for 7-11 worms. (Note: the errorbars are too small to be visible in the bottom plot). Both parameters decrease with increasing viscosity.

Chapter 4

Discussion

Our results show that swimming and crawling are not distinct locomotory behaviors and depend on the mechanical load of the environment. Because it has been hypothesized that swimming and crawling are controlled by different circuits, we expected a sharp transition, but our results suggest that there is at most one neural circuit that is modulated by the environmental mechanical load.

Ultimately we would like to answer how the oscillatory locomotion is controlled in the neural circuit – is there a CPG and if so, which neurons participate on the network, and how does mechanosensation provide feedback? Because the anatomy of *C. elegans* is simple, it is feasible that the circuitry can be mapped out using a combination of theoretical models, genetic tools, and laser ablation techniques.

Many theoretical models for crawling have been proposed, but these models only account for the crawling behavior observed on agar surfaces [22] [23]. One of the difficulties of forming theoretical models for *C. elegans* in fluids is due to their size. The forces that act on a body that is immersed in fluid is characterized by the Reynolds number N_R , the ratio between the inertial forces and the viscous forces acting on the body [23]:

$$N_R = \frac{Lv\rho}{\mu}, \quad (10)$$

where L = physical dimensions of the body, ρ = density of the liquid, and μ = viscosity of the liquid. Because *C. elegans* are approximately 1 mm in length in 100 μ M in diameter, they have a N_R of order unity in water, meaning both viscous forces and inertial forces play a significant role in the dynamics of the worms. For comparison, typical flagellum in water have N_R of order 10^{-3} , meaning the internal forces can be ignored, and typical fish in water have N_R of order 10^4 , meaning viscous forces can be ignored [23]. Because both viscous and internal forces are important in *C. elegans*, creating a model that takes these factors into account is difficult. Thus, theoretical models for the CPG for forward locomotion have been for worms crawling on surfaces.

Since the connectivity between all neurons has been established, current models use this wiring diagram in an attempt to find the neural circuitry for the locomotion. For example, Karbowski, et al. [22] and Niebur and Erdos [23] propose a CPG that is initiated in the head neurons. Bryden and Cohen [24] showed that it is possible for the locomotory gait to not have a CPG and still be oscillatory. They propose a subcircuit that integrates sensory information and outputs the undulating locomotion.

Although this model does not expand to describe swimming behavior, it gives insight on another possible mechanism for *C. elegans* locomotion.

From the experimental side, forward genetics has yielded many mutants that are deficient in locomotion, mechanosensation, or neuromodulation. These worms provide more information for which neurons play a role in locomotion and sensory feedback (See Appendix). Laser ablation, the killing of a neuron using a laser [25], for specific target neurons will also provide insight on the neural circuit of locomotion.

Our results show that mechanical load plays an integral part of *C. elegans* locomotion. The worms adapt to their environment by changing the wavelength and the frequency of undulation. Our analysis provides direction for theoretical models to produce both swimming and crawling behavior, and provides a paradigm for exploring mutants or laser-ablated worms.

Chapter 5

Appendix

5.1 Dextran solution

To ensure that the non-Newtonian aspect of our hypromellose solution does not affect the qualitative locomotory behavior, we are currently testing worms in a solution of dextran (Sigma) in 10mM hepes buffer. Solutions with high concentrations of dextran unfortunately have high osmolality. The worms are typically grown on an agar plate with 21 mM NaCl (200mOsmol). When these worms are placed in a hyperosmotic solution of 200mM NaCl, their body volume shrinks to 70% of their original volume within a minute after being placed in the solution. Worms placed in even more hyperosmotic solutions of 300mM – 500mM NaCl are not able to survive the osmotic shock [19].

To acclimate the worms to high osmolality conditions, worms were grown on agar plate with 200mM NaCl for a few days before exposure to the solutions. Worms grown on high-salt plates adapt by producing more glycerol and are able to survive in solutions up to 500mM NaCl [19]. To keep the change in volume constant across all solutions, we balanced our solutions with sorbitol (Sigma), a type of sugar alcohol, to match the highest osmolality (40% dextran in 10mM hepes buffer, 632 mmol/kg).

The viscosity measurements are shown in Figure 5-1. Although at low concentrations of dextran, the viscosity changes as a function of shear rate, at higher concentrations of dextran, the viscosities are constant. We are currently gathering data of the locomotory behavior of the worms in these solutions.

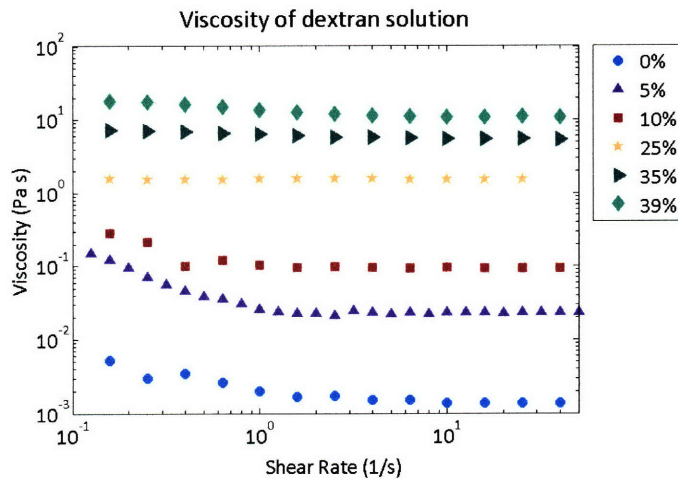


Figure 5-1 Viscosity of dextran solution
 Except at low percentages, the viscosity stays constant as a function of shear rate.

5.2 Mutants

To further understand the role of sensory feedback, we are in progress of carrying out the assay in various mutant worms. Currently we are observing 4 mutant worms. The mutant *mec-4(d)* (MECHANOSENSORY abnormality), is a worm that is insensitive to gentle mechanical stimuli. The mutant *trp-4* (TRANSIENT RECEPTOR POTENTIAL channel) is also insensitive to gentle mechanical stimuli and is believed to have abnormalities in the stretch-receptor-mediated proprioception. The mutant *cat-2* (abnormal CATEcholamine distribution) (n4517) has abnormalities in dopamine² levels and is known to be slow in locomotory response to food. The mutant *tph-1* (TRYPTOPHAN HYDROXYLASE) (n46221) worms have abnormalities in serotonin³ biosynthesis and are claimed to have metabolic and behavioral processes similar to starved worms. Information about mutant worms can be found at WormBase [26].

Preliminary results are shown in Figure 5-2. The means for each mutant are for $n = 1$ to 5 worms. For comparison, the wildtype N2 from the previous section is also shown. No obvious differences are observed but more study is needed.

² Dopamine is a neuromodulator.

³ Serotonin is a neuromodulator and a neurotransmitter.

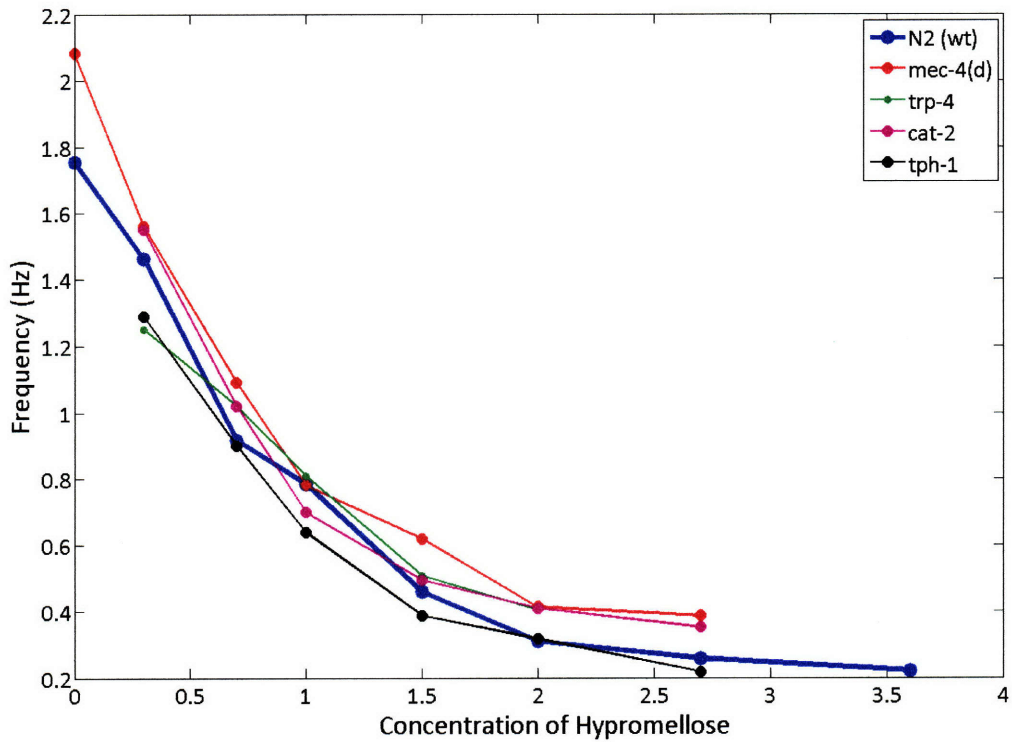
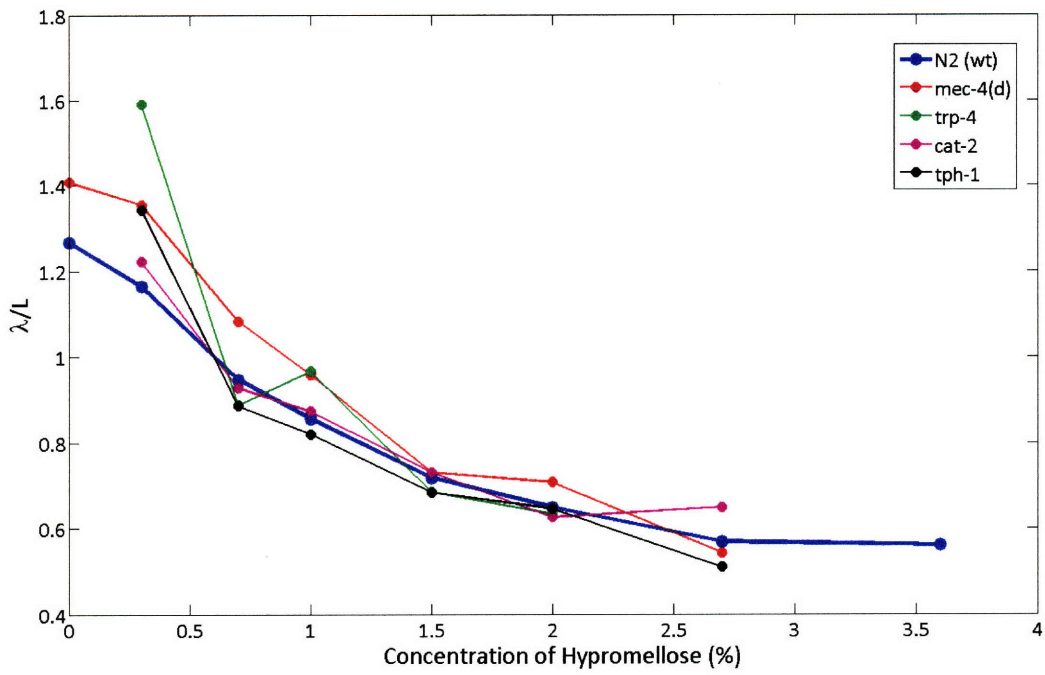


Figure 5-2 Top: Mean normalized wavelength of undulations for mutants. Bottom: Mean frequency of undulations for mutants.

Error bars are excluded for clarity. Note that this is only preliminary data and $n = 1$ to 5 worms (except for N2 – same as previous section).

Chapter 6 Bibliography

- [1] *Central pattern generators*. **Hooper, Scott**. R176-R177, s.l. : Elsevier Science, March 2000, Current Biology, Vol. 10.
- [2] *Principles of rhythmic motor pattern generation*. **Marder, E. and Calabrese, RL**. 3, July 1996, Physiol. Rev., Vol. 76, pp. 687-717.
- [3] *Mechanisms of Gastric Rhythm Generation in the Isolated Stomatogastric Ganglion of Spiny Lobsters: Bursting Pacemaker Potentials, Synaptic Interactions, and Muscarinic Modulation*. **Elson, R. and Selverston, A**. 3, September 1992, Journal of Neurophysiology, Vol. 68.
- [4] *A central pattern generator underlies crawling in the medicinal leech*. **Eisenhart, FJ, Cacciatore, TW and Kristan, WB Jr**. 7-8, s.l. : Springer, Jul-Aug 2000, J Comp Physiol, Vol. 186.
- [5] *Neuronal Generation of the Leech Swimming Movement*. **Stent, GF, et al**. 4348, June 23, 1978, Science, Vol. 200, pp. 1348-1357.
- [6] **Hooper, Scott**. Central Pattern Generators. *Encyclopedia of Life Sciences*. s.l. : John Wiley & Sons, 2006.
- [7] **Altun, Z.F. and Hall, D.H**. *WormAtlas*. [Online] 2002-2006. <http://wormatlas.org/>.
- [8] *Wiring optimization can relate neuronal structure and function*. **Chen, Beth, David, Hall and Chklovskii, Dmitri**. 12, march 21, 2006, PNAS, Vol. 103, pp. 4723-4728.
- [9] **Altun, Z.F. and Hall, D.H**. Handbook of C. elegans Anatomy. *WormAtlas*. [Online] 2005. <http://www.wormatlas.org/handbook/contents.htm>.
- [10] **Riddle, DL, et al**. *C. Elegans II*. Plainview : Cold Spring Harbor Laboratory Press, 1997.
- [11] *The genetics of Caenorhabditis elegans*. **Brenner, S**. 1, May 1974, Genetics, Vol. 77, pp. 71-94.
- [12] Benecel. Wilmington, DE, USA : Hercules Incorporated, Aqualon Division.
- [13] **Sulston, J. and Hodgkin, J**. Methods. *The Nematode Caenorhabditis elegans*. W. B. Wood. Cold Spring Harbor : Cold Spring Harbor Press, 1988, pp. 587-606.
- [14] *An Introduction to Rheology*. Great Britain : Michelle Press, 1997. International Federation of Societies of Cosmetic Chemists.
- [15] **Wilkinson, W.L**. *Non-Newtonian Fluids: Fluid Mechanics, Mixing and Heat Transfer*. New York : Pergamon Press, 1960.
- [16] **Pipkin, A.C**. *Lectures on Viscoelasticity Theory*. 2nd Edition. New York : Springer-Verlag, 1986. Vol. 7.
- [17] **Dinger, Dennis**. *Rheology for Ceramics*. Kearney : Morris Publishing, 2002.
- [18] AR500/1000 Hardware Manual. New Castle : TA Instruments, 2000.

- [19] *Adaptation of the nematode Caenorhabditis elegans to extreme osmotic stress.* **Lamitina, S.T., et al.** April 2004, *Am J Physiol Cell Physiol*, Vol. 286.
- [20] *Evolutionarily conserved WNK and Ste20 kinases are essential for acute volume recovery and survival after hypertonic shrinkage in Caenorhabditis elegans.* **Choe, Keith and Strange, Kevin.** s.l. : C915-C927, 2007, *Am J Physiol Cell Physiol*, Vol. 293.
- [21] *Mechanosensation and mechanical load modulate the locomotory gait of swimming C. elegans.* **Korta, J., et al.** s.l. : Company of Biologists, April 2007, *Journal of Experimental Biology*, Vol. 210, pp. 2383-2389.
- [22] *Systems level circuit model of C. elegans undulatory locomotion: mathematical modeling and molecular genetics.* **Karbowski, J., et al.** s.l. : Springer Science, 2008, *J Comput Neurosci*, Vol. 24, pp. 253-276.
- [23] *Theory of the locomotion of nematodes: Dynamics of undulatory progression on a surface.* **Niebur, E. and Erdos, P.** 5, 1991, *Biophysical Journal*, Vol. 60.
- [24] *Neural control of Caenorhabditis elegans forward locomotion: the role of sensory feedback.* **Bryden, J. and Cohen, N.** s.l. : Springer-Verlag, 2008, *Biol Cybern*, Vol. 98, pp. 339-351.
- [25] **Bargmann, CI and Avery, L.** Laser killing of cells. [ed.] HF Epstein and DC Shakes. *C. elegans: Modern Biological Analysis of an Organism.* New York : Academic Press, pp. 225-250.
- [26] *WormBase web site.* [Online] <http://www.wormbase.org>. WS170.
- [27] *Development of swimming in the medicinal leech, the gradual acquisition of a behavior.* **French, K.A., et al.** 9, s.l. : Springer, September 2005, *J Comp Physiol*, Vol. 191. 0340-7594.
- [28] *Rhythmic Swimming Activity in Neurones of the Isolated Nerve Cord of the Leech.* **Kristan, WB, Jr. and Calabrese, RL.** 1976, *J. Exp. Biol*, Vol. 65, pp. 643-668.